Oxygen ordering and strain-related morphology in $YBa_2Cu_{3-x}M_xO_7$ systems, where M is a trivalent atom

Zhi-Xiong Cai, Yimei Zhu, and D. O. Welch
Materials Science Division, Department of Applied Science, Brookhaven National Laboratory, Upton, New York 11973
(Received 1 April 1992)

Monte Carlo simulations were performed on an anisotropic lattice-gas model which well represents the interactions between oxygen atoms in $YBa_2Cu_3O_7$ systems doped with trivalent impurity atoms M such as Fe or Al. Concentration wave amplitudes obtained from these simulations were used to calculate the diffuse x-ray scattering intensity caused by the resulting displacement field using a concentration-wave–displacement-wave approach, and the results are compared with x-ray and electron diffraction data. The results suggest that the small orthorhombic domains (short-range ordering) associated with the oxygen "cross-links" around impurity atoms M cause the diffuse scattering intensity to fall off with the scattering wave-vector difference $\mathbf{q}$ from a Bragg peak as $1/q^2$ for small q and as $1/q^4$ for larger q. We show that the average size of such domains can be obtained from diffuse x-ray scattering data.

I. INTRODUCTION

Extensive Monte Carlo simulations using an anisotropic-lattice-gas-model potential have been performed[1–4] to describe oxygen ordering in $YBa_2Cu_3O_7$ and related systems and seem to describe reasonably well the experimental data on the structural phase diagram,[4] the orthorhombic-to-tetragonal phase transition in the Fe-doped system, and the metastable structure of quenched samples.[3] It is also found that the lattice-gas model can provide a good approximation for kinetic phenomena such as oxygen diffusion. However, because these lattice-gas models treat the oxygen atoms as particles on a rigid lattice, they cannot explain without modification the microstructures of the $YBa_2Cu_3O_7$ system caused by elastic distortion of the lattice, such as the formation of "tweed" in the $YBa_2Cu_{3-x}Fe_xO_7$ system.[6,7]

On the other hand, continuum elasticity theory has been an excellent model to study the lattice deformation due to oxygen ordering, as shown by the work of Semenovskaya and Khachaturyan.[5] Using the concentration-wave–displacement-wave approach, Jiang *et al.*[8] showed that the calculated spectrum of the diffuse x-ray scattering for the $YBa_2Cu_{3-x}Al_xO_7$ system agrees very well with their experimental data in the long-wavelength limit. At shorter wavelengths, however, the local fluctuations of oxygen concentration become an important factor, thus detailed information on oxygen concentration waves is needed to evaluate the diffuse scattering intensity.

In this paper, we try to combine the merits of both of these two approaches so that the whole spectrum of diffuse x-ray scattering can be characterized. If we assume that the interactions between oxygen atoms are predominantly screened Coulomb interactions, the energy associated with the lattice distortion is thus much smaller than the energy associated with the redistribution of oxygen between different lattice sites, since the latter results in a much larger deviation of the oxygen-atom positions from their ideal positions. Therefore, the elastic energy can be treated as a perturbation of the lattice-gas Hamiltonian. We will use the oxygen-atom configuration obtained from our Monte Carlo simulation of the lattice-gas model on a rigid square lattice as the input concentration wave amplitude for continuum elasticity theory calculations. In essence, we assume that the oxygen distribution over lattice sites is not affected by the orthorhombic distortion of the lattice. In light of the excellent agreement between previous results calculated based on the lattice-gas model and experimental results, this is a reasonable assumption.

In Sec. II, we will review briefly the lattice-gas model suitable for $YBa_2Cu_{3-x}M_xO_7$ (where M is a trivalent atom such as Fe or Al) and Monte Carlo simulation results. In Sec. III, we describe the calculation of the diffuse scattering intensity using continuum elasticity theory.

II. OXYGEN ORDERING ON A RIGID LATTICE

First, let us review briefly the lattice-gas model for the $YBa_2Cu_{3-x}M_xO_7$ system. This model is based on the assumption that the interaction between oxygen atoms can be approximated by a metallically screened Coulomb interaction on a rigid lattice.[3] Since the $YBa_2Cu_3O_{7-\delta}$ system is metallic for $0<\delta<0.5$, this assumption seems reasonable for oxygen concentrations within that range. In addition to the Coulomb repulsion, two oxygen atoms bridged by a Cu atom also experience a short-range attractive interaction due to covalent bonding.

The structure of the CuO basal plane is approximated by a two-dimensional square lattice consisting of Cu atoms, oxygen atoms, and oxygen vacancies (V), as shown in Fig. 1. When a divalent or monovalent Cu ion is replaced by an impurity ion M such as Fe or Al, an extra hole will tend to localize near the M sites, i.e., the M ion becomes effectively trivalent. This will have two major effects: (a) the binding energy of an oxygen ion near

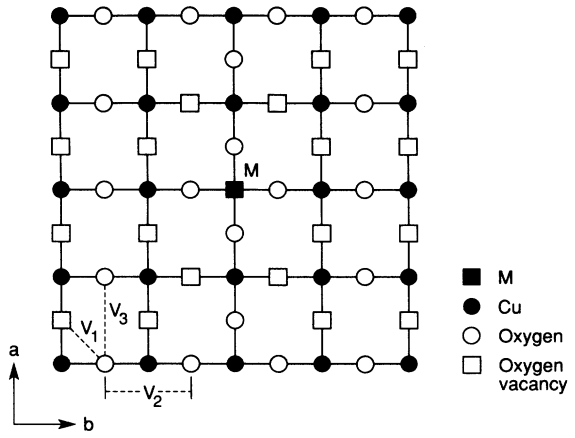

FIG. 1. Structure of the basal plane of $YBa_2Cu_{3-x}M_xO_7$ with a single M impurity. V_1 is the interaction parameter between nearest-neighbor oxygen atoms, V_2 is the interaction parameter between next-nearest-neighbor oxygen atoms bridged by Cu, and V_3 is the interaction parameter between next-nearest-neighbor oxygen atoms not bridged by Cu. The values of V_1 and V_3 depend upon whether the oxygen atoms are near an M impurity (see text).

the M site increases; and (b) the repulsion between oxygen atoms near the M site increases, either due to the increase of the negative charge of oxygen ions or due to the decrease in local screening because of the decrease in the concentration of mobile holes.

Based on this picture, as shown in Fig. 1, the Hamiltonian representing the M-doped 1:2:3 system is[3]

$$H=\sum_{\langle ij\rangle} V_{1ij}n_in_j+V_2\sum_{(ij)b} n_in_j + \sum_{(ij)a} V_{3ij}n_in_j+\sum_i E_in_i \ , \tag{1}$$

where the following interaction parameters were used in the calculations:

$$V_2=-0.2 \text{ eV} \tag{2}$$

and

$$V_{1ij}=0.25 \text{ eV}, \quad V_{3ij}=0.1 \text{ eV} \ , \tag{3}$$

if neither site i nor site j is a nearest neighbor of M,

$$V_{1ij}=0.5 \text{ eV}, \quad V_{3ij}=0.2 \text{ eV} \ , \tag{4}$$

if either site i or site j is a nearest neighbor of M and the other site is not, and

$$V_{1ij}=1.0 \text{ eV}, \quad V_{3ij}=0.4 \text{ eV} \ , \tag{5}$$

if both sites i and j are nearest neighbors of M. In addition, the single-site binding energy $E_i=-4$ eV if site i is the nearest neighbor of M and $E_i=0$ otherwise. n_i is the oxygen occupational operator ($n_i=1$ if site i is occupied by an oxygen atom and $n_i=0$ if site i is an oxygen vacancy site).

Figure 1 shows the oxygen configuration which is found near a single impurity atom M. By minimizing energy we find that the impurity atom forces the oxygen to form short Cu-O chains along the a axis thus forming a local "cross-link" around the impurity site.

Experimentally, the distribution of M ions is found to be uniform in samples prepared using the sintering procedure.[6] We therefore assume that the M atoms randomly occupy Cu sites.

Monte Carlo (MC) simulations were performed with Kawasaki dynamics using this lattice-gas model. Lattice sizes ranging from 32×32 to 100×100 with periodic boundary conditions were used. The high-temperature configuration was obtained by performing a MC simulation at $T=2300$ K (well above the oxygen order-disorder phase transition temperature for all the systems concerned), and the system was equilibrated at this temperature with 10 000 MCS/site (MCS is Monte Carlo steps). The low-temperature configurations were obtained by lowering the temperature of the system to 300 K in steps of 100 K. 2000 to 10 000 MCS/site were used to obtain thermodynamic averages for each temperature.

Figure 2 shows a typical oxygen and M configuration of $YBa_2Cu_{2.9}M_{0.1}O_7$ with a random M distribution. The local "cross-links" formed around the M atoms disrupt the orthorhombic structure, and overall the system shows tetragonal symmetry. Since the oxygen atoms can be regarded as interstitial in CuO planes causing expansion of the lattice parameter in the direction of the Cu-O chain and contraction perpendicular to the Cu-O chain, the resulting lattice distortion caused by the "cross-links" is along the (110) and ($\bar{1}$10) directions. High-resolution

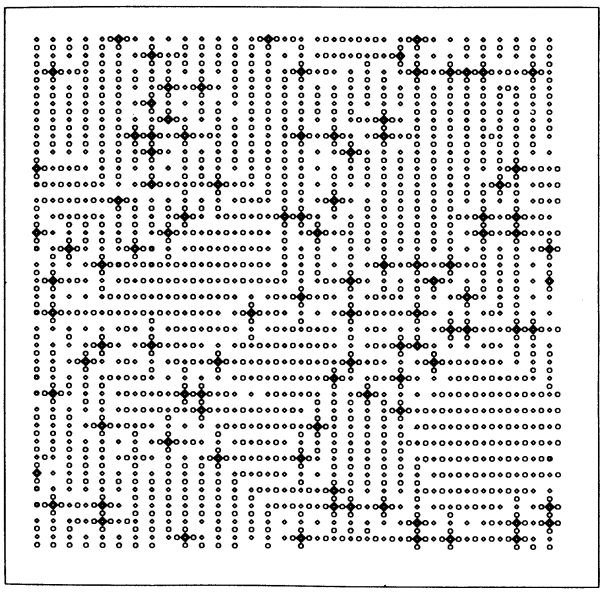

FIG. 2. A configuration of the $YBa_2Cu_{3-x}M_xO_7$ basal plane for $x=0.1$ obtained by a Monte Carlo simulation of a 32×32 lattice with periodic boundary conditions at 300 K. The M impurity is randomly distributed. The small diamonds indicate Cu positions, the small circles indicate oxygen positions, and the large diamonds indicate M positions.

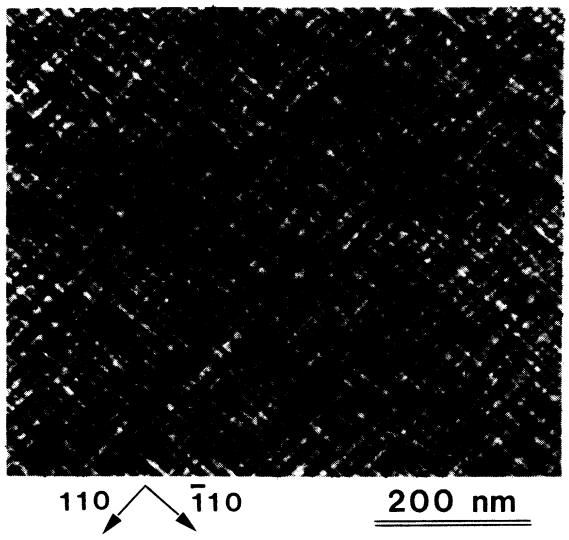

FIG. 3. Multibeam transmission electron microscope image of tweed morphology in $YBa_2Cu_{3-x}Fe_xO_7$ with $x=0.1$.

electron-microscopy and transmission electron-microscopy (TEM) image analysis show that these (110) and ($\bar{1}10$) shear displacements are responsible for the tweed contrast (see, for example, Fig. 3).[6]

III. DIFFUSE SCATTERING DUE TO LATTICE DISTORTION AND THERMAL VIBRATION

Since the displacements of oxygen atoms in the orthorhombic domains, relative to the square lattice, are small, a linear elastic approximation can be used to study the lattice distortion due to oxygen ordering in the $YBa_2Cu_{3-x}M_xO_7$ system. In the long-wavelength limit, the displacement of the lattice site s can be written to first order as follows[8,9]

$$\delta\mathbf{R}_s=\sum_{\mathbf{q}}\mathbf{A}_{\mathbf{q}}c_{\mathbf{q}}\exp(-i\mathbf{q}\cdot\mathbf{R}_s)\ , \tag{6}$$

where $c_{\mathbf{q}}$ is the amplitude of the planar oxygen concentration wave with wave vector $\mathbf{q}$. $\mathbf{A}_{\mathbf{q}}$ is determined by three inhomogeneous linear equations:

$$q\lambda_{ijlm}n_jn_l A_{\mathbf{q}m}=\lambda_{ijlm}n_jL_{lm}\ , \tag{7}$$

where a summation is made over repeated indices; λ_{ijlm} is a component of the elastic modulus tensor; n_i is a component of the unit vector $\mathbf{n}=\mathbf{q}/q$; $L_{lm}=\delta u_{lm}/\delta c_0$, where u_{lm} is a component of the strain tensor; and c_0 is the average oxygen concentration of the CuO basal plane. For tetragonal crystals, the tensor components L_{lm} are given by

$$L_{lm}=\frac{1}{d_l}\frac{\partial d_l}{\partial c_0}\delta_{lm}\ , \tag{8}$$

where d_l is the lattice constant. In the present paper we treat the oxygen atoms in the basal plane of $YBa_2Cu_{3-x}M_xO_7$ as interstitial in a square Cu lattice where the interstices are midpoints of the edges (x and y) of the unit cell. The tensor components are

$$L^x_{11}=\frac{1}{b}\frac{\partial b}{\partial c_0},\quad L^x_{22}=\frac{1}{a}\frac{\partial a}{\partial c_0}\ , \tag{9}$$

$$L^y_{11}=L^x_{22},\quad L^y_{22}=L^x_{11}\ , \tag{10}$$

$$L^x_{22}=L^y_{33}=\frac{1}{c}\frac{\partial c}{\partial c_0}\ , \tag{11}$$

where a,b,c are the lattice constants of the $YBa_2Cu_3O_7$ system, with an oxygen concentration in the Cu-O basal plane of c_0. If we treat the oxygen atoms in the Cu-O plane as interstitial in a square lattice, Eq. (7) may then be modified as

$$q\lambda_{ijlm}n_jn_l A^{\gamma}_{\mathbf{q}m}=\lambda_{ijlm}n_jL^{\gamma}_{lm},\quad \gamma=x,y\ . \tag{12}$$

Once $\mathbf{A}_{\mathbf{q}}$ is obtained from the above equation, the intensity of the diffuse scattering due to lattice distortion for a small displacement $\mathbf{q}$ of the scattering vector away from a reciprocal-lattice point (Bragg peak) $\mathbf{Q}$ can be derived from the following expression:[9]

$$I_H(\mathbf{Q}+\mathbf{q})=|F(\mathbf{Q})|^2|\mathbf{Q}\cdot(\mathbf{A}^x_{\mathbf{q}}c^x_{\mathbf{q}}+\mathbf{A}^y_{\mathbf{q}}c^y_{\mathbf{q}})|^2\ , \tag{13}$$

where $c^x_{\mathbf{q}}$ and $c^y_{\mathbf{q}}$ are the amplitudes of the oxygen concentration wave of two different kinds of interstitial oxygen atoms (along the b and a axes, respectively) and $F(\mathbf{Q})$ is the atomic structure factor of the full unit cell.

The thermal average of the diffuse scattering intensity can then be obtained as

$$\begin{aligned}\langle I\rangle_H&=\langle I(\mathbf{Q}+\mathbf{q})\rangle/|F(\mathbf{Q})|^2\\&=|\mathbf{Q}\cdot\mathbf{A}^x_{\mathbf{q}}|^2\langle|c^x_{\mathbf{q}}|^2\rangle+|\mathbf{Q}\cdot\mathbf{A}^y_{\mathbf{q}}|^2\langle|c^y_{\mathbf{q}}|^2\rangle\\&\quad+|(\mathbf{Q}\cdot\mathbf{A}^{*x}_{\mathbf{q}})(\mathbf{Q}\cdot\mathbf{A}^y_{\mathbf{q}})|\langle c^{*x}_{\mathbf{q}}c^y_{\mathbf{q}}\rangle\\&\quad+|(\mathbf{Q}\cdot\mathbf{A}^{*y}_{\mathbf{q}})(\mathbf{Q}\cdot\mathbf{A}^x_{\mathbf{q}})|\langle c^{*y}_{\mathbf{q}}c^x_{\mathbf{q}}\rangle\ ,\end{aligned} \tag{14}$$

where the correlation functions of $c^x_{\mathbf{q}}$ and $c^y_{\mathbf{q}}$ are obtained by the Fourier transform of $\langle|c^x(\mathbf{r})|^2\rangle$, $\langle|c^y(\mathbf{r})|^2\rangle$, and $\langle|c^{*x}(\mathbf{r})c^y(\mathbf{r})|\rangle$, which are obtained from the Monte Carlo simulation for a 100×100 lattice averaged over 10 different distributions of M atoms. The subscript H denotes the fact that this scattering intensity comes from a generalized Huang scattering.[9] Following Jiang *et al.*[8] we chose $c_0=0.5$, $L^x_{11}=-L^x_{22}=0.011$, $L^x_{33}=0.010$, and the values of λ_{ijlm} to be those given by Reichardt *et al.*[10] for the $YBa_2Cu_3O_7$ compound.

Since the most diffuse scattering experiments are performed at room temperature, the thermal diffuse scattering (TDS) can also make a major contribution to the total diffuse scattering intensity. To the first-order approximation[11]

$$I_{\mathrm{TDS}}=|F(\mathbf{Q})|^2\frac{kT}{\tau}\frac{(\mathbf{Q}+\mathbf{q})^2}{q^2}K(f)_g\ , \tag{15}$$

where T is the temperature, τ is the volume of the unit cell,

$$K(f)_g=g_ig_m(\lambda_{ijlm}f_jf_l)^{-1}\ , \tag{16}$$

and $\{g\}$ and $\{f\}$ are the wave normals of $\mathbf{Q}$ and $\mathbf{q}$, respectively. The total diffuse scattering intensity is then the sum of the thermal and Huang diffuse scatterings, $I=I_H+I_{\mathrm{TDS}}$.

Figures 4(a)–4(i) show the diffuse scattering intensity, calculated as described above, compared with the diffuse scattering data obtained by transmission electron microscopy of $YBa_2Cu_{3-x}Fe_xO_7$ for $x=0.09$. Figures 4(a)–4(c) show the calculated diffuse scattering intensity I_H due to lattice distortion, and Figs. 4(d)–4(f) show the calculated total difuse scattering intensity I due to both lattice distortion and thermal diffuse scattering. Figures 4(g)–4(i) show the diffuse scattering data obtained by TEM. The theoretical diffuse scattering intensity profile agrees very well with the TEM data. This indicates that it is reasonable to assume that the lattice distortion due to oxygen ordering is of the same order of magnitude as the thermal vibration of the lattice. Were the lattice distortion very large compared to the thermal vibration amplitude, I_H would have dominated the diffuse scattering intensity profile, thus the TEM data in Figs. 4(g)–4(i) would have the characteristics of Figs. 4(a)–4(c), which is not observed here. The diffuse patterns are streaked along the two equivalent (110) directions in reciprocal space for $\mathbf{Q}=(h00)$ or $(0h0)$, while for $(hh0)$, one set of the (110) streaks (the radial streaks) vanishes. Around $(hk0)$, $h\neq k\neq 0$, the intensity and the length of the streaks depend on the distance from the origin.[7] The characteristic features of the simulated diffuse scattering intensity, which arises from $(110)/(\bar{1}10)$ shear displacements of the crystal due to oxygen distribution, are consistent with the electron diffuse scattering, tweed image[6] as shown in Fig. 3, and the x-ray diffuse scattering observations.[8] The qualitative features of the calculated diffuse scattering data agree with the results of Jiang *et al.*,[8] who use a similar approach but assume that the oxygen atoms are distributed randomly. We have also calculated the diffuse scattering for other M concentrations and find that they are all qualitatively similar as long as the Cu-O chains in both directions are present. In other words, the qualitative features of the "tweed" pattern yield no information about the local domain structure caused by the M doping since it is dominated by the scattering of long wavelengths (small q). Quantitative study of the diffuse scattering intensity further away from the Bragg peak is required.

Figure 5 shows the calculated diffuse scattering intensity due to lattice distortion for various M concentrations, compared with the x-ray diffuse scattering intensity for $YBa_2Cu_{3-x}Al_xO_7$, where $x=0.14$.[8] In the long-wavelength limit (where the wavelength is much larger than the domain size), the displacement wave is determined by the orientation of orthorhombic "microdomains." Here the term "microdomains" means a region where the orthorhombic short-range order exists (as can be seen in Fig. 2 of the short Cu-O chains). The domain size indicates the correlation length of such short-range order. Since the location and orientation of the orthorhombic microdomains are in turn determined by the cross-links of Cu-O chains around M atoms, and since they are randomly distributed throughout the sample, the diffuse scattering in the long-wavelength limit shows the characteristics of Huang scattering, i.e., $I\propto 1/q^2$. The main difference between our results and those of Jiang *et al.* is that, compared with a random distribution of oxygen defects, we now have a lower concentration of defects (or scattering centers) but with much stronger displacement fields, since the defects consist of

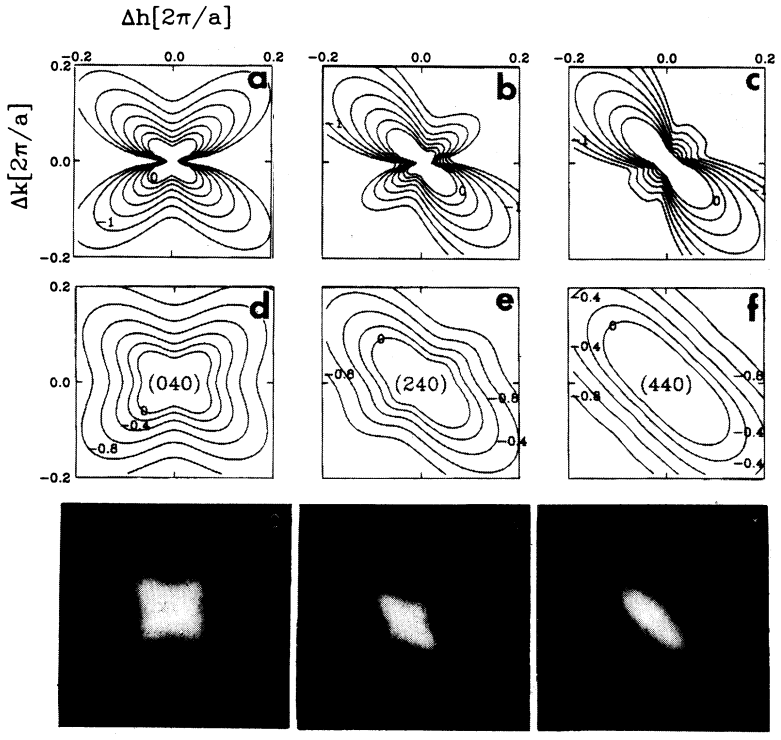

FIG. 4. (a)–(c) Contour plots in logarithmic intervals of the diffuse scattering intensity of $YBa_2Cu_{3-x}M_xO_7$ due to lattice distortion for $x=0.1$, around (a) (040), (b) (240), and (c) (440) reciprocal-lattice points. (d)–(f) Contour plots in logarithmic intervals of the total diffuse scattering intensity of $YBa_2Cu_{3-x}M_xO_7$ for $x=0.1$, around (d) (040), (e) (240), and (f) (440) reciprocal-lattice points. (g)–(i) Diffuse scattering measured by TEM spectroscopy of $YBa_2Cu_{3-x}Fe_xO_7$ for $x=0.09$, around (g) (040), (h) (240), and (i) (220) reciprocal-lattice points.

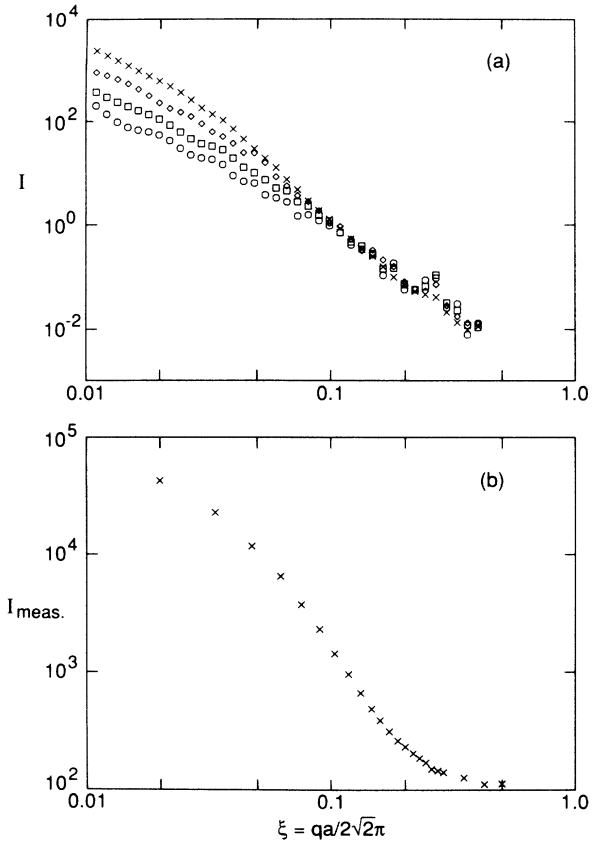

FIG. 5. (a) Calculated diffuse scattering intensity (in arbitrary units) of $YBa_2Cu_{3-x}M_xO_7$ for $x=0.05$ ($\times$), 0.1 ($\diamond$), 0.15 ($\square$), 0.2 ($\circ$), vs reduced wave vector $\xi=qa/2\sqrt{2}\pi$ in the $(\bar{1}10)$ direction at the (660) point in reciprocal lattice. (b) Measured x-ray diffuse scattering intensity of $YBa_2Cu_{3-x}Al_xO_7$ for $x=0.14$ vs reduced wave vector $\xi=qa/2\sqrt{2}\pi$ in the $(\bar{1}10)$ direction at the (660) point (Ref. 8). Note that we have not attempted to normalize the theoretical intensity at $q=0$ to the experimental value since it varies from sample to sample.

the orthorhombic microdomains. Because of the larger size of the defects, the region of the Huang scattering is restricted to smaller q values, where the scattering is governed by the displacement field far away from the defect centers. For larger q values (i.e., shorter wavelength), c_q is no longer a constant (i.e., independent of q). In fact, the results suggest that $\langle |c_q^2| \rangle \propto 1/q^2$, which results in a decrease of diffuse scattering intensity proportional to $1/q^4$. The minimum q value where the $1/q^4$ scattering is observed gives a critical radius $R_{crit}=1/q_c$, which is the distance from the center of an orthorhombic microdomain where the displacement $\delta\mathbf{R}_s$ is so large $\mathbf{q}\cdot\delta\mathbf{R}_s \simeq 1$. Near the Bragg peak with low Miller indices, R_{crit} is approximately the average size of the orthorhombic microdomain. This relation can be used for an estimate of the domain size. We find that when x increases from 0.05 to 0.20, the size of the orthorhombic microdomains decreases from 80 to 10 Å. Unfortunately, the small lattice size of the system we used in the Monte Carlo simulation made the transition from Huang's scattering to $1/q^4$ scattering not as sharp as was observed in experiment (see Fig. 5), especially in the case of high-M content.

It should be emphasized that the orthorhombic microdomains shown in this paper are quite different from the microtwinning structure of the quenched $YBa_2Cu_3O_{7-\delta}$ systems shown by the simulation of Semenovskaya and Khachaturyan,[5] which has sharp antiphase domain walls (twins). The domain structure we find in our Monte Carlo simulation is short-range order with very thick domain walls.

IV. SUMMARY

In conclusion, we have shown that, based on the assumption that the interaction between oxygen atoms in $YBa_2Cu_{3-x}M_xO_7$ is predominantly a screened Coulomb interaction, the elastic distortion of the lattice can be treated as a perturbation of the two-dimensional lattice-gas model. The diffuse scattering data obtained by this technique are in good quantitative agreement with the results of TEM and x-ray scattering experiments. We showed that the "tweed" contrast observed in TEM can be explained by the short-range oxygen ordering which can be described as small orthorhombic microdomains, the size of which is determined by the Cu-O chain cross-links around M impurities. From quantitative measurements of x-ray diffuse scattering profiles, the average size of the orthorhombic microdomains can be obtained.

ACKNOWLEDGMENTS

We would like to thank Professor S. C. Moss, Dr. P. Wochner, and Professor A. G. Khachaturyan for stimulating discussions. This work is supported by the U.S. Department of Energy, Division of Materials Sciences, Office of Basic Energy Sciences under Contract No. DE-AC02-76CH00016. The computer simulation was performed on the Cray X-MP at NERSC, Lawrence Livermore National Laboratory.

[1]D. de Fontaine, L. T. Wille, and S. C. Moss, Phys. Rev. B **36**, 5709 (1987).
[2]Zhi-Xiong Cai and S. D. Mahanti, Solid State Commun. **67**, 287 (1988).
[3]Zhi-Xiong Cai and S. D. Mahanti, Phys. Rev. B **40**, 6558 (1989).
[4]D. de Fontaine, M. E. Mann, and G. Ceder, Phys. Rev. Lett. **63**, 1300 (1989).
[5]S. Semenovskaya and A. G. Khachaturyan, Phys. Rev. Lett. **67**, 2223 (1991).
[6]Yimei Zhu, M. Suenaga, and A. R. Moodenbaugh, Philos. Mag. Lett. **62**, 51 (1990).
[7]Yimei Zhu, M. Suenaga, and J. Tafto, Philos. Mag. Lett. **64**, 29 (1991).
[8]X. Jiang, P. Wochner, S. C. Moss, and P. Zschack, Phys. Rev. Lett. **67**, 2167 (1991).
[9]M. A. Krivoglaz, *Theory of X-ray and Thermal Neutron Scattering by Real Crystals* (Plenum, New York, 1969).
[10]W. Reichardt, L. Pintschovius, B. Hennion, and F. Collin, Supercond. Sci. Technol. **1**, 173 (1988).
[11]W. A. Wooster, *Diffuse X-ray Reflections From Crystals* (Clarendon, Oxford, 1961).

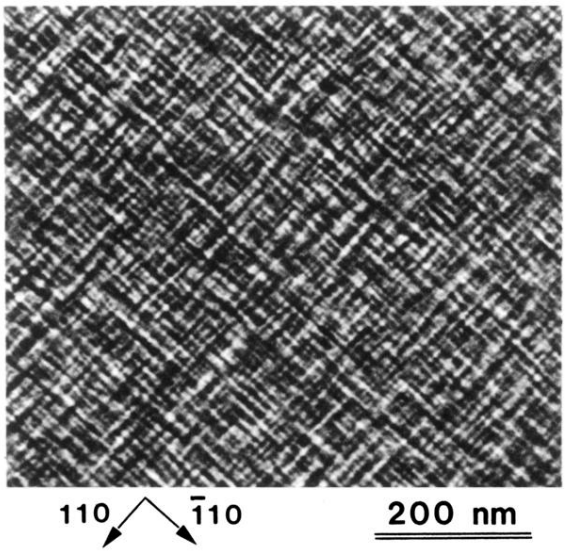

FIG. 3. Multibeam transmission electron microscope image of tweed morphology in $YBa_2Cu_{3-x}Fe_xO_7$ with $x=0.1$.

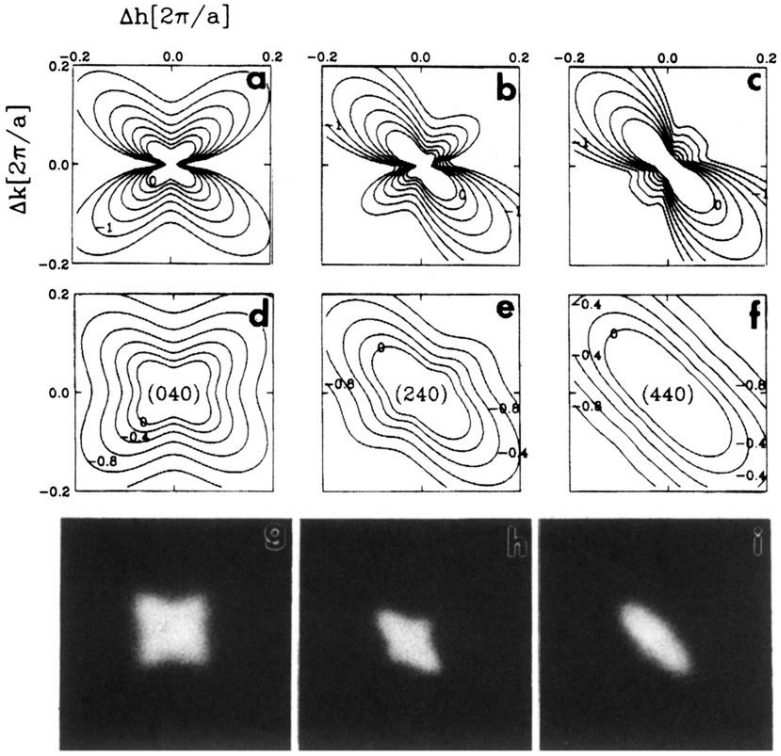

FIG. 4. (a)–(c) Contour plots in logarithmic intervals of the diffuse scattering intensity of $YBa_2Cu_{3-x}M_xO_7$ due to lattice distortion for $x=0.1$, around (a) (040), (b) (240), and (c) (440) reciprocal-lattice points. (d)–(f) Contour plots in logarithmic intervals of the total diffuse scattering intensity of $YBa_2Cu_{3-x}M_xO_7$ for $x=0.1$, around (d) (040), (e) (240), and (f) (440) reciprocal-lattice points. (g)–(i) Diffuse scattering measured by TEM spectroscopy of $YBa_2Cu_{3-x}Fe_xO_7$ for $x=0.09$, around (g) (040), (h) (240), and (i) (220) reciprocal-lattice points.